

Extraction of centre line from curvilinear objects

J. ROKICKI¹, V. MATIUKAS¹, A. UŠINSKAS¹, and R. ADAŠKEVIČIUS²

¹Department of Electronic Systems, Vilnius Gediminas Technical University, 41 Naugarduko Str., LT-03227 Vilnius, Lithuania

²Department of Ergonomics, Kaunas Technological University, 3 JSC Elintos Prietaisai Terminalo Str., LT-54469 Kaunas District, Lithuania

This tutorial paper surveys three methods designed to detect the centre line in curvilinear structures. These are the iterative thinning, Steger's and derivatives' methods. We aim to illustrate the effectiveness of the chosen methods for processing laser-trace images and magnetic resonance slices of human head. The essence of each three methods is presented and important parameters are discussed. Experiments have been carried out and results are discussed in the light of the quality of the centre line produced and work time of all three methods.

Keywords: laser centre line, skeletonization, centre line extraction, Gaussian kernel, thinning, derivatives, Hessian matrix.

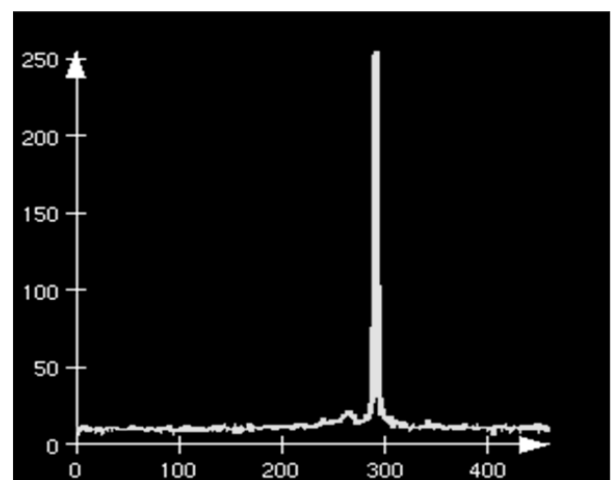
1. Introduction

Extraction of the centre line is an important issue in many digital image processing operations. The centre line can be used to extract information about roads and rivers contained in an aerial photography, or to determine parameters used in medical imaging, such as the shortest path between points in a blood vessel angiogram. It is also used in 3D scanning, where an object is scanned by a laser beam and at the same time pictured by a camera. Reconstruction is performed from the data recorded by the camera (Fig. 1). Determining the boundary of the scanned object poses a challenge, although the laser beam's profile usually has a Gaussian distribution (Fig. 2), but due to reflections from surfaces and varying absorption coefficients in different parts of the object surface, the laser trace may take rather unexpected shapes in captured pictures [1]. Thus, the object is often represented in a picture by a line of varying brightness and width (bigger than one pixel).

A natural decision is choosing the centre points of a line. Intuitively, we can define the centre line as a line that splits an object into two equal parts. However, as most of real objects are asymmetrical, true equality is hard to achieve. Alternatively, the centre line can be defined as the medial axis, i.e., a set of centre points of maximal disks inscribed into the object. By maximal we mean that it is not described by any of the other disks belonging to that object. The medial axis is expected to give the exact centre of the line. In our case, however, we manipulate greyscale images instead of objects having predefined boundaries. Thus, our method aims to extract the ridge points, i.e., the local max-



(a)



(b)

Fig. 1. An image recorded by 3D scanner camera (a) and profile of laser line (b).

* e-mail: rokicki@gmail.com

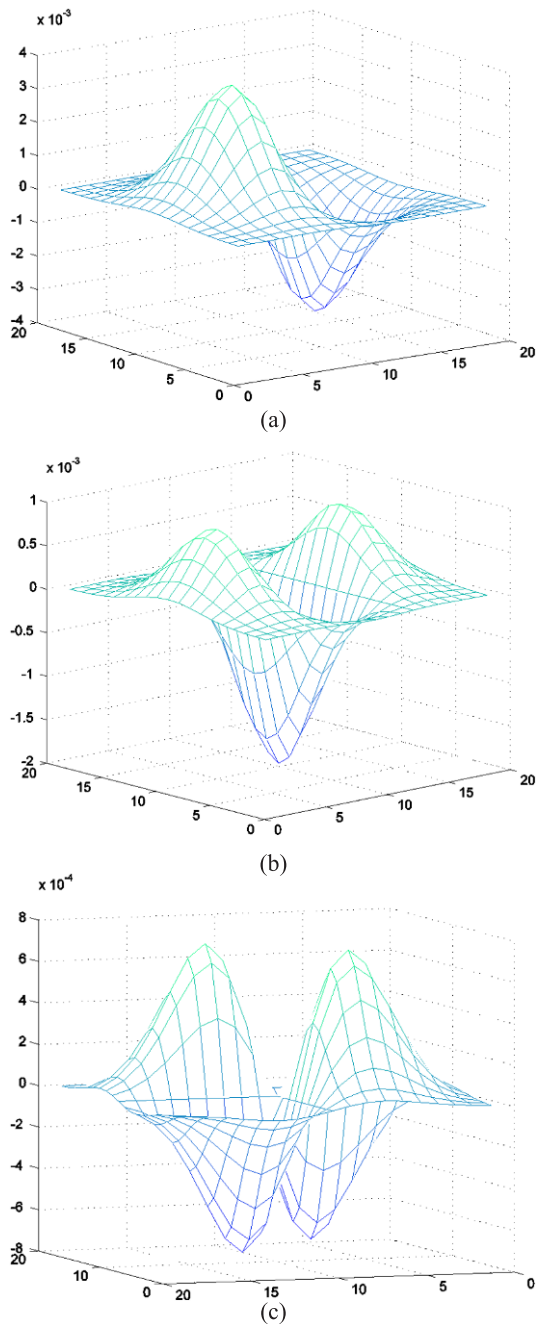


Fig. 2. Gaussian kernels: (a) $g_{x,\sigma}(x, y)$, (b) $g_{xx,\sigma}(x, y)$, and (c) $g_{xy,\sigma}(x, y)$.

ima in the direction of primary curvature. We aim, these ridge points to possess the following set of properties:

- smoothness – the detected points should not deviate too much from the centre of the real curve. The second derivative is evaluated, while moving along the centre line. Its value represents the alternation of the centre points. High values of the second derivative would indicate high curvature of the centre line,
- continuity – the centre line cannot have discontinuities (even a gap one pixel wide is not allowed),
- centredness – the centre line cannot approach the line boundaries,

- thinness – the centre line should be one pixel wide, and for each line, only a single centre line can exist,
- connectivity – sequencing the pixels is important.

In this tutorial, we discuss three different methods for extraction of the centre line: the thinning method (based on morphological operations), the Steger's method, and the derivatives' method (based on the image convolution with Gaussian kernels).

2. Methods

2.1. Thinning method

Thinning is erosion of white-line pixels so that an object without holes erodes to a minimally connected stroke located equidistantly to its nearest outer boundaries. An object with holes erodes to a minimally connected ring midway between each hole and its nearest outer boundaries [2].

Pixels can be removed using one of two approaches, sequential and parallel. In the sequential approach, a pixel is removed depending on the result of the previous pixel deletion. That makes next pixel to be a function of the current pixel change (and all the previous pixels) [3]. Meanwhile, in the parallel approach, all pixels are processed simultaneously in one iteration. Parallel algorithms can be further subdivided into fully parallel and partially serialized by introducing some subiterations (when pixels are processed side by side, examining object in the directions north, west, east, and south). Parallel algorithms are considered superior in comparison to sequential ones, as the latter cannot preserve the connectivity criterion when 3×3 mask is used [4]. Possible solutions to this problem include using a bigger mask or performing subiterations. Thinning algorithms operate only on binarized images. An additional thresholding step has to be introduced, which segments an object (in our case, the laser trace) from the background. It is not difficult, since the laser trace is much lighter than dark background.

We use the parallel approach to extract the centre line [5]. To outline the algorithm, some words have to be said about the topology. In two dimensions we consider two cases of connectivity:

- 8-connectivity, when all the pixels $[x_1, x_8]$ are adjacent to the centre pixel p (Fig. 3).
- 4-connectivity, when we take into account only x_1, x_3, x_5, x_7 .

The proposed algorithm returns the centre line, which is said to be 8-connected. The pixel p is deleted if three conditions are satisfied:

x_4	x_3	x_2
x_5	p	x_1
x_6	x_7	x_8

Fig. 3. Neighborhood of the point p .

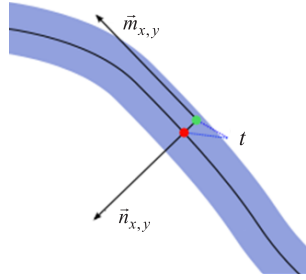


Fig. 4. Points of the centre line moved along the direction perpendicular to the line $\vec{n}_{x,y}$.

- $X_H(p) = 1$, if the number of crosses from an object ($x_i = 1$) to the background ($x_i = 0$), is given by

$$b_i = \begin{cases} 1, & \text{if } (x_{2i-1} = 0 \text{ and } x_{2i+1} = 1) \\ 0, & \text{otherwise} \end{cases} \quad (1)$$

- $2 < \min\{n_1(p), n_2(p)\} < 3$, (2)

where

- $n_1(p) = \sum_{i=1}^4 x_{2k+1} \cup x_{2k}$ (3)

- $n_2(p) = \sum_{i=1}^4 x_{2k} \cup x_{2k+1}$ (4)

is the representation of 4-adjacent pairs of pixels.

- $(x_2 \cup x_3 \cup \bar{x}_8) \cap x_1 = 0$ (5)

for the first iteration and its rotation by 180° in the second iteration.

2.2. The Steger's line extraction method

The purpose of this method is extracting the centre line with subpixel precision using convolution of the image function and Gaussian kernels. The method can detect lines in one-dimensional (1D) as well as two-dimensional (2D) spaces.

2.2.1. Detection of lines in 1D

For the one-dimensional image $I(x)$ with the line profile close to a parabolic form, determining the first derivative $I'(x)$ is sufficient. The point at which $I'(x)$ reduces to zero corresponds to the centre line. To select salient lines, the second derivative $I''(x)$ has to be computed. Salient lines are represented by the magnitude of $I''(x)$ at the point where $I'(x)$ reduces to zero. Bright lines on a dark background will have $I''(x) < 0$, whereas dark lines on a bright background will accordingly have $I''(x) > 0$ [6].

In practice, images contain a significant amount of noise. For that reason, it is necessary to convolve the image with derivatives of the Gaussian kernel given by [7]

$$g_\sigma(x) = \frac{1}{\sqrt{2\pi}\sigma} e^{-x^2/2\sigma^2}, \quad g'_\sigma(x) = \frac{-x}{\sqrt{2\pi}\sigma^3} e^{-x^2/2\sigma^2}, \quad (6)$$

$$g''_\sigma(x) = \frac{x^2 - \sigma^2}{\sqrt{2\pi}\sigma^5} e^{-x^2/2\sigma^2},$$

where σ denotes the standard deviation of x .

2.2.2. Detection of lines in 2D

Curvilinear structures in 2D are modelled as structures having a line profile similar to the 1D case in the direction perpendicular to that of the line. This perpendicular direction is denoted by $n(t)$. So, the first directional derivative should become zero, and the second derivative should obtain a large absolute value in the direction of $n(t)$ [8]. To ensure that the image can be differentiated at every point, it is convolved with the Gaussian kernels.

Then, direction perpendicular to the line $n(t)$ is computed.

The first step is to create the kernels (Fig. 2) to be convolved with the image

$$\begin{aligned} g_{x,\sigma}(x, y) &= g_\sigma(y)g'_\sigma(x) \\ g_{y,\sigma}(x, y) &= g'_\sigma(y)g_\sigma(x) \\ g_{xx,\sigma}(x, y) &= g_\sigma(y)g''_\sigma(x) \\ g_{xy,\sigma}(x, y) &= g'_\sigma(y)g'_\sigma(x) \\ g_{yy,\sigma}(x, y) &= g''_\sigma(y)g_\sigma(x) \end{aligned} \quad (7)$$

where $g_\sigma(x)$ and $g_\sigma(y)$ correspond to the Gaussian distribution along the x and y axis, $g'_\sigma(x)$, $g'_\sigma(y)$, and $g''_\sigma(x)$, $g''_\sigma(y)$ are their first and second derivatives, and σ denotes the standard deviation that depends on the line's thickness. It is recommended to choose σ such that

$$\sigma = \frac{w}{\sqrt{3}} \quad (8)$$

where w is the line's width in pixels. The perpendicular direction is obtained after convolution of the image with the corresponding Gaussian kernel $r_x, r_y, r_{xx}, r_{xy}, r_{yy}$ [7]

$$\begin{aligned} r_x &= g_{x,\sigma}(x, y) * I(x, y), \\ r_y &= g_{y,\sigma}(x, y) * I(x, y), \\ r_{xx} &= g_{xx,\sigma}(x, y) * I(x, y), \\ r_{xy} &= g_{xy,\sigma}(x, y) * I(x, y), \\ r_{yy} &= g_{yy,\sigma}(x, y) * I(x, y), \end{aligned} \quad (9)$$

where $I(x, y)$ denotes the image, $g_{xx,\sigma}, g_{xy,\sigma}, g_{yy,\sigma}$ are the Gaussian kernels, $r_x, r_y, r_{xx}, r_{xy}, r_{yy}$ is convolution response or partial derivatives [8].

The perpendicular direction $n(t)$ is computed by constructing a Hessian matrix and computing its eigenvectors and eigenvalues

$$H(x, y) = \begin{bmatrix} r_{xx} & r_{xy} \\ r_{xy} & r_{yy} \end{bmatrix} \quad (10)$$

After calculating the matrix for each point in the image, the eigenvalues and eigenvectors are extracted. The eigenvector with the largest absolute eigenvalue is chosen as the one representing the perpendicular direction to the line. The eigenvector's length is normalized so that $\|n_x, n_y\|_2 = 1$.

The exact ridge point $p(x,y)$ is evaluated by approximating the image with a quadratic polynomial at the selected location (x_0,y_0) given by

$$p(x,y) = r(x_0,y_0) + r_x(x_0,y_0)x + r_y(x_0,y_0)y + \frac{1}{2}r_{xx}(x_0,y_0)x^2 + r_{xy}(x_0,y_0)xy + \frac{1}{2}r_{yy}(x_0,y_0)y^2, \quad (11)$$

where the x and y coordinates are expressed as a shift along the two orthogonal vectors n_x and n_y in the direction of maximum gradient from the analyzed point (x_0, y_0) . Thus, $x = n_x t$ and $y = n_y t$. This way, only one unknown t remains. It determines the amount of movement in the direction of n_x and n_y needed to reach the maximum point. For this, we have to determine the point where $p(x,y)$ is maximal, or to determine the location where the first derivative of the polynomial is equal to zero

$$\frac{d}{dt} p(tn_x, tn_y) = 0. \quad (12)$$

This gives us the solution $t = -\frac{a}{b}$, when $b \neq 0$, where

$$a = r_x n_x + r_y n_y, \quad (13)$$

$$b = r_{xx} n_x^2 + 2r_{xy} n_x n_y + r_{yy} n_y^2.$$

For a point to belong to the centre line, it should stay within pixel boundaries, which are given by

$$[p_x, p_y] \in \left[-\frac{1}{2}, \frac{1}{2}\right] \times \left[-\frac{1}{2}, \frac{1}{2}\right], \quad (14)$$

where

$$[p_x, p_y] = (tn_x, tn_y). \quad (15)$$

Here, t represents displacement of a point along the direction vector $n = [n_x, n_y]$ (Fig. 4). To select only the salient lines, we can use the second directional derivative along n .

2.3. The derivatives' method

This method was proposed by Koller *et al.* [9]. The derivatives' algorithm is based on non-linear combination of linear filters. The algorithm searches for elongated, symmetric line structures, while suppressing the response to line edges. The filter uses two shifted kernels of the first-order Gaussian derivatives combined in a non-linear way.

A simple derivative of the image function does not suffice as it is often not sensitive to lines of different width. As an alternative, Canny in Ref. 10 proposed using the second derivative of a Gaussian function to be convolved with the image. This alternative, however, suffered from such effects as unwanted extremes of the convolution near the edges of the line profile.

The basic idea behind the derivatives' method is similar to the approach presented in Ref. 11, but it is extended to 2D. Furthermore, with minor modifications, it can be applied to curvilinear structures in 3D space.

2.3.1. Detection of centre line in 1D

The derivatives' method was shown to work well on different line profiles, but we will use a bar-shaped line profile for simplicity

$$f_B(x) = \Theta\left(x + \frac{w}{2}\right) - \Theta\left(x - \frac{w}{2}\right), \quad (16)$$

$$\Theta(x) = \begin{cases} 1, & x > 0 \\ 0, & \text{else} \end{cases}, \quad (17)$$

where $f_B(x)$ is the bar profile centred at $x = 0$ with its height equal to 1 and the width w .

The centre line extraction filter R_s is based on a non-linear combination of the shifted left and right edge detectors

$$R_s(x) = \min\{P[(E_l * f_B)(x)], P[(E_r * f_B)(x)]\}, \quad (18)$$

$$E_l = -G'_\sigma(x + \sigma), \quad (19)$$

$$E_r = -G'_\sigma(x - \sigma),$$

where $E_l(x)$ and $E_r(x)$ denote the left and right edge detectors, correspondingly, $G'_\sigma(x) = -xe^{-x^2/2\sigma^2}$ is the first derivative of the Gaussian function, σ is the standard deviation of x , $P(x)$ denotes the positive part of x .

The response of the left and right edge detectors to a bar-shaped profile is shown in Fig. 5(a). Non-linear combination of responses gives a sharp peak at the centre of the profile $x = 0$, Fig. 5(b). Standard deviation should be chosen as large as possible, but not bigger than $0.5w$ to keep the filter inside the line. It is proved that for a line of width w , the line detector has a maximum at the centre of the profile ($x = 0$) when $\sigma = 0.42w$ [9].

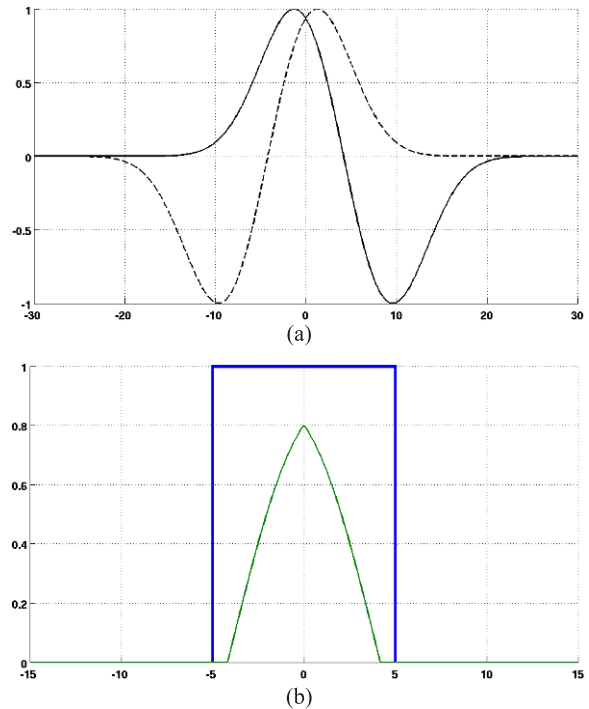


Fig. 5. Response of the left $[E_l(x)]$ and the right $[E_r(x)]$ edge detectors to a bar-shaped profile (a) and non-linear combination of responses gives a sharp peak at centre of the profile ($x = 0$) (b).

2.3.2. Detection of centre line in 2D

Our current implementation of the filter uses 2D kernels; otherwise it is analogous to the 1D case [14]. Filtering as a detection function is applied in the direction $\vec{d}_o = (\cos \alpha, \sin \alpha)$ of the profile that is orthogonal to the line direction \vec{d}_l . A scaled Gaussian function and its derivatives in x and y directions are used to implement the left and right edge detectors

$$\begin{aligned} E_{lx}(x, y) &= -G'_{x,\sigma}(x + \sigma, y), \\ E_{ly}(x, y) &= -G'_{y,\sigma}(x, y + \sigma), \\ E_{rx}(x, y) &= -G'_{x,\sigma}(x - \sigma, y), \\ E_{ry}(x, y) &= -G'_{y,\sigma}(x, y - \sigma), \end{aligned} \tag{20}$$

where $G'_{x,\sigma}$ and $G'_{y,\sigma}$ are the first-order derivatives of the 2D Gaussian function in the x and y directions, respectively.

The filtering procedure can be applied in several ways. One possibility is using an iterative approach for a discrete number of directions to select the direction with the maximal response [12,13]. Another approach is calculating the local orientation of the line structure (similar to the Stegers' method), and then filter can be steered to this direction.

Centre line points of the curvilinear structure are extracted using non-maximum suppression by detecting local maxima in the direction \vec{d}_o [14].

3. Results

To validate the results, we created a synthetic image shown in Fig. 6(a). The image consists of two objects, a circle and a rectangle. The circle has sharp edges and bright pixel values. In comparison, the edges of the rectangle are less sharp (blurred out). The centre line was determined manually and is shown in Fig. 6(a) by a black line. Extracted centre lines are indicated by darker lines (red color). Only iterative thinning was able to extract the line without any discontinuities, Fig. 6(b). Note that due to the lack of subpixel extraction, the pixels do not always coincide with the centre line determined manually. Therefore, the only method capable to extract the centre line with subpixel precision was the Stegers' method [Fig. 5(a)]. None of the methods used in this study could determine correctly the position of the centre line at locations with sudden turns.

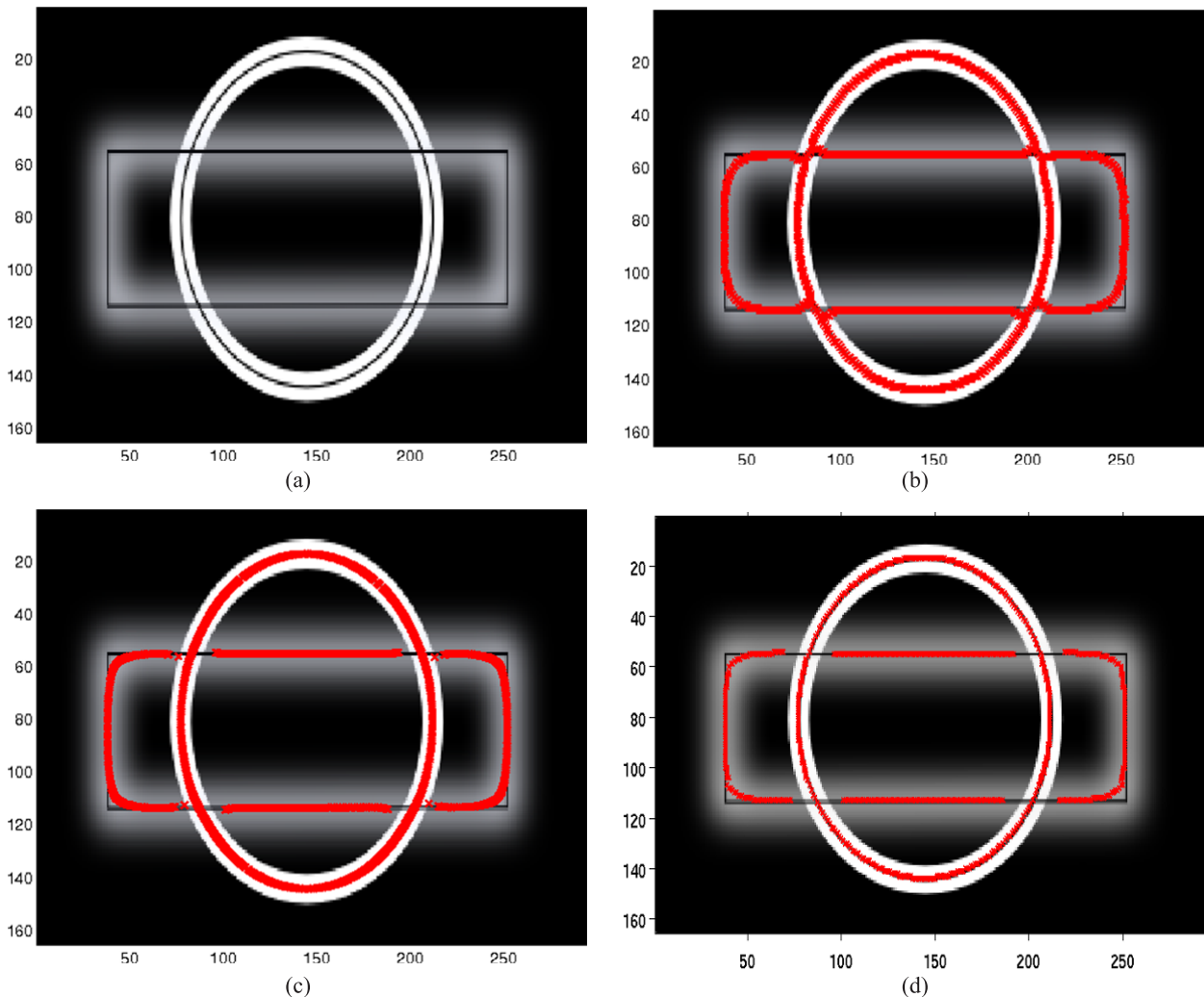


Fig. 6. Centre line extraction from synthetic image (a), by thinning (b), Steger's (c), and derivatives' method (d).

For further testing different pictures were used. The results with three of them are presented in this paper. Two of them originate as images made by three dimensional (3D) scanner (image of the laser trace) and the third one is an MRI slice of the human brain. Two different objects were scanned, namely: a cylinder [Fig. 7(a)] and a square box [Fig. 7(b)]. The size of all images is different and varies from 267×200 for the cylinder image to 635×635 for the MRI slice [Fig. 7(c)]. The third image was chosen due to its complex nature – numerous lines and bifurcations. All lines in the images are bright and lie on a dark background. Number of the centre line points and the execution time for each

method were measured. We shall discuss the properties of smoothness, continuity, centredness, thinness, and connectivity. All the methods were implemented in the *MATLAB* environment. The speed of algorithm was evaluated using a PC with a dual-core Intel Pentium 2.16 GHz processor (2 GB of RAM). The results are presented in Table 1.

Of all the three methods presented here, the thinning method was found to be the fastest one. However, this method lacks subpixel precision. The extracted centre line has the smallest number of points in comparison to the other methods. An additional thresholding step is needed to binarize the picture. Sometimes gaps between pixels occur,

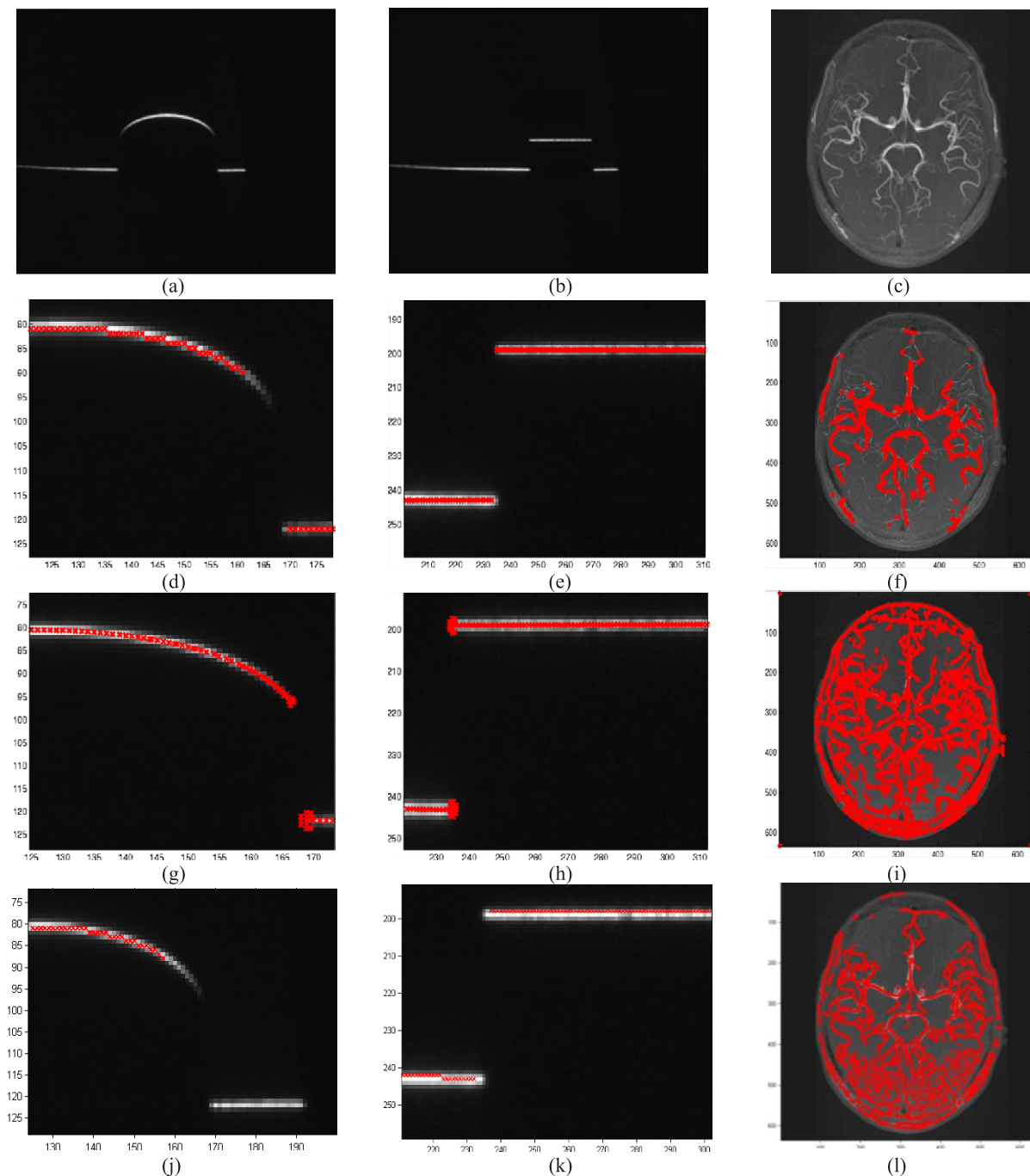


Fig. 7. Original pictures (a), (b), (c); centre line extracted by using thinning (d), (e), (f); Steger's (g), (h), (i); and derivatives' methods (j), (k), (l).

Table 1. Comparison of execution times for different methods.

No	Size	Thinning		Steger's		Derivatives'	
		Time (s)	Points	Time (s)	Points	Time (s)	Points
1	267×200	0.02	129	1.16	255	4.2	162
2	533×400	0.05	331	7.29	459	17.7	396
3	635×635	0.12	2950	22.45	15344	63.6	6734

which is not acceptable. Results obtained using this method are presented in Fig. 7(d), 7(e), and 7(f). No point connection is preserved, but the centre line is always one pixel wide. This method works only with binary images, so the results are influenced by the threshold value selected.

As seen in Fig. 7(g), 7(h), and 7(i), the Steger's method allows extracting the points of the centre line with subpixel precision. However, now, the centre line is not always represented by a single point (sometimes two neighbouring points indicate that the centre of a line is in the opposite one). Also, additional points appear at the endlines [Fig. 8(b)], but generally the centre line is one pixel wide. Another drawback of this method is that it cannot detect correctly the centre line when two objects are too close [Fig. 8(b)]. In such cases, a smaller value of σ should be chosen. There are no gaps between line points as well. The method depends heavily on the value of the parameter σ , which was chosen to be equal to 2 in the current experiment. The bigger value of σ would lead to wrong detection of the centre line; too small value of σ tends to yield two centre lines instead of a single line. Moreover, small branches occur at the line ends. The points are not connected. To connect them, a separate procedure needs to be developed. On the positive side, the Steger's method is quite resistant to noise (due to convolution with Gaussian kernels), it can work with grey-scale images directly.

In its current implementation, the derivatives' method was found to be the slowest (see Table 1.) The results of using this method are affected by the line width selected. Smaller values tend to increase the number of points detected. On the other hand, the number of false positives increases accordingly. Selecting a bigger value for the line width leads to filtering out the thinner lines [Fig. 7(j)]. In the current study, the line width was chosen to be 6 pixels.

Moreover, the derivatives' method does not return any connectivity information. Therefore, the centre line detected has discontinuities, as seen in Fig. 8(c). Nevertheless, it returns a single pixel for the width of the centre line. The derivatives' method works well on endlines [Fig. 7(j)] if [Fig. 7(k)] compared to the Steger's method [Fig. 7(g)] and [Fig. 7(h)].

In closely zoomed-in Figs. 8(a) and 8(b), the thinning and Steger's methods tend to select the centre of the line closer to the inner boundaries of intersecting blood vessels.

The derivatives' method also has a potential of delivering subpixel accuracy. It performs reasonably with graphs during inner operations, as seen in Fig. 5.

The biggest advantage of this method is that it requires only one parameter, namely σ , proportional to the line width.

4. Conclusions

The iterative thinning method is more than 100 times faster than either the Steger's, or the derivatives' methods. Its main disadvantage is inability to return the centre line with subpixel accuracy. The method produces gaps in the centre line and is not suitable for complex images.

The Steger's method is much slower due to convolution of the image function with the corresponding kernel functions, and calculation of the eigenvector. But the method is capable of computing points of the centre line with subpixel accuracy. The main disadvantage of the Steger's method is that it sometimes fails to return the correct position of the centre line when objects are close to each other. Also, additional points are left at the endlines.

The Steger's method is very sensitive to parameter values. The centre line extraction is affected heavily by the choice of values for two different parameters: the kernel

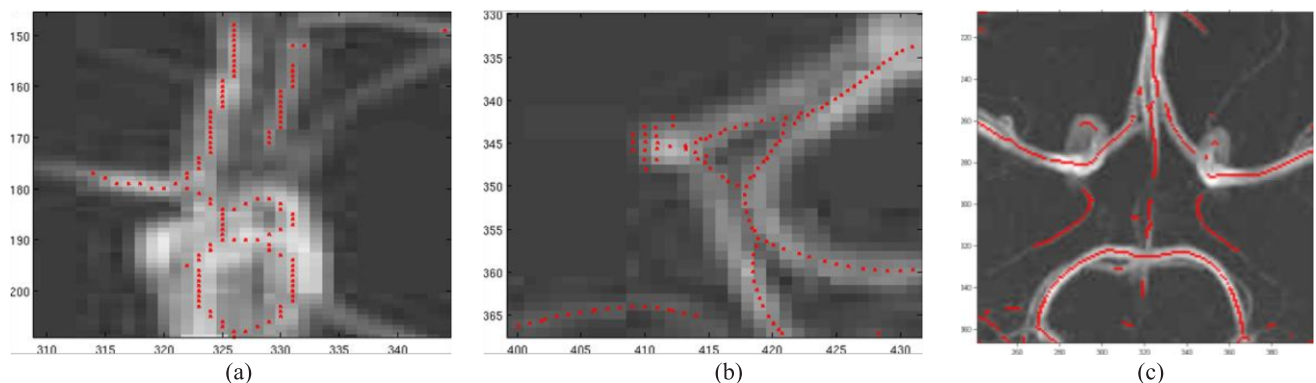


Fig. 8. The most common problems using thinning (a), Steger's (b), and derivatives' methods (c).

width, as determined by σ , and the level of the line saliency, depending on the threshold value of the second directional derivative selected.

Another disadvantage of the Steger's method is that precision of extracting the centre line depends greatly upon σ . Inaccurate selection of σ can lead to wrong detection of the centre line (if σ is too big), or can produce two centre lines (if σ is chosen smaller than the line width).

The derivatives' method is the slowest of all the three methods investigated.

The derivatives' method disregards connectivity and continuity in some cases. This tends to produce small gaps in the centre line detected.

Acknowledgements

This paper was supported by the Lithuanian State Science and Studies Foundation (contract No. G-55/07).

References

1. O. Mendoza-Yero and J. Alda, "Irradiance map of an apertured Gaussian beam affected by coma", *Optics Commun.* **271**, 517–523 (2007).
2. W.K. Pratt, *Digital Image Processing*, John Wiley & Sons, 2nd edition, New York, 1991.
3. R.C. Staunton, "One-pass parallel hexagonal thinning algorithm", *IEE P-Vis. Image Sign.* **148**, 45–53 (2001).
4. L. Lam and C.Y. Suen, "[An evaluation of parallel thinning algorithms for character recognition](#)", *IEEE T. Pattern Anal.* **17**, 914–919 (1995).
5. L. Lam, S. Lee, and C.Y. Suen, "Thinning methodologies-A comprehensive survey", *IEEE T. Pattern Anal.* **14**, 869–885 (1992).
6. C. Steger, "Extraction of curved lines from images", *Proc. 13th Int. Conf. on Pattern Recognition*, 251–255 (1996).
7. C. Steger, "Subpixel-precise extraction of lines and edges", *International Archives of Photogrammetry and Remote Sensing*, 141–156 (2000).
8. C. Steger, "[An unbiased detector of curvilinear structures](#)", *IEEE T. Pattern Anal.* **20**, 113–125 (1998).
9. T.M. Koller, G. Gerig, G. Szekely, and D. Dettwiler, "Multi-scale detection of curvilinear structures in 2-D and 3-D image data", *ICCV '95: Proc. 5th Int. Conf. on Computer Vision*, 864–869 (1995).
10. J.F. Canny, "Finding edges and lines in images", *Technical Report 720*, MIT Artificial Intelligence Laboratory, 1983.
11. J.B. Subirana-Vilanova and K.K. Sung, "Ridge-detection for the perceptual organization without edges", *Proc. 4th Int. Conf. on Computer Vision*, 57–64 (1993).
12. W.T. Freeman and E.H. Adelson, "[The Design and use of steerable filters](#)", *IEEE T. Pattern Anal.* **13**, P. 891–906 (1991).
13. W. Freeman and E.H. Adelson, "Steerable filters for early vision, image analysis and wavelet decomposition", *Proc. 3rd Int. Conf. on Computer Vision, ICCV'90*, IEEE Computer Society, 406–415 (1993).
14. J. Canny, "A computational approach to edge detection", *IEEE T. Pattern Anal.* **8**, 679–698 (1986).